Acta Neurobiol. Exp. 2001, 61: 157-174

Unbiased high resolution method of EEG analysis in time-frequency space

Katarzyna J. Blinowska and **Piotr J. Durka**

Laboratory of Medical Physics, Institute of Experimental Physics, Warsaw University, 69 Hoża St., 00-681 Warsaw, Poland, Email: kjbli@fuw.edu.pl

Abstract. Matching Pursuit (MP) - a method of high-resolution signal analysis - is described in the context of other methods operating in time-frequency space. The method relies on an adaptive approximation of a signal by means of waveforms chosen from a very large and redundant dictionary of functions. The MP performance is illustrated by simulations and examples of sleep spindles and slow wave activity analysis. An improvement of the original procedure, relying on the introduction of stochastic dictionaries, is proposed. A comparison of the performance of dyadic and stochastic dictionaries is presented. MP with stochastic dictionaries is characterized by an unmatched resolution in time-frequency space; moreover it allows for parametric description of all (periodic and transient) signal features in the framework of the same formalism. Matching pursuit is especially suitable for analysis of non-stationary signals and is a unique tool for the investigation of dynamic changes of brain activity.

Key words: time-frequency, non-stationary signals, matching pursuit, EEG, sleep spindles

INTRODUCTION

EEG (electroencephalogram) reflects electrical activity of a multitude of neural populations in the brain. This signal is extremely complex, since EEG is generated as a superposition of different simultaneously acting dynamical systems. The oscillatory activity of neuronal pools reflected in characteristic EEG rhythms constitutes a mechanism by which the brain can regulate changes of state in selected neuronal networks to cause qualitative transitions between modes of information processing (Lopes Da Silva 1996).

The complex character of the EEG and its significance in brain research and clinical practice caused the early introduction of signal analysis methods to EEG studies. Spectral methods of EEG processing can be traced back to the first attempt to use Fourier analysis to analyze the EEG in 1932 (Dietsch 1932). The Fast Fourier transform (FFT) was applied to the EEG soon after its introduction, and until today spectral analysis remains the most widespread signal processing method in this field. Limitations of FFT promoted the introduction of parametric methods such as autoregressive (AR) or autoregressive - moving average (ARMA) models, free from windowing effects.

Development of non-linear methods of signal analysis brought an explosion of work concerning the application of chaotic formalisms to the EEG (Basar and Bullock 1989, Dvorák and Holden 1991). Work of Freeman, based on carefully planned physiological experiments, brought new insights into the mechanisms of non-linear modes of brain operation (Skarda and Freeman 1987). However, applying chaos theory to the EEG proved to be more difficult than was expected. It has been shown that linear forecasting of signals from human and animal brains is as good as, and sometimes better than non-linear predictions (Blinowska and Malinowski 1991). Tests of non-linear procedures, performed on surrogate (phase disturbed) data, revealed their failure to describe different kinds of EEG time series (Pijn et al. 1991, Achermann et al. 1994).

In view of the evidence presently available, application of typical methods of non-linear time series analysis, such as calculation of attractor dimension or Ljapunov coefficients, seems to be fully justified only for special cases such as epileptic EEG (Pijn et al. 1991) or activity of a group of neurons in a well defined operation mode (Skarda and Freeman 1987). This fact is not surprising when we consider the multitude of dynamic processes running in brain and their ever-changing character.

All the above mentioned methods, linear and non-linear, assume stationarity of the signal - in spite of the fact that information processing by the brain is mostly reflected in fast dynamic changes of its activity. This fact suggests that the application to the analysis of EEG and LFP (local field potentials) of methods operating in time-frequency space brings the substantial progress.

The first method which allowed for the time-frequency representation of a signal's energy distribution was windowed Fourier transform (WFT). It relies on an estimation of power spectra (by Fourier transform) for short time windows, shifted along the time axis.

Widespread application of time-frequency methods of signal analysis started in eighties with Wavelet Transform (WT), which describes a signal in terms of coefficients $\{c_{s,u}\}$ representing the signal's energy content in a specified time-frequency region. This representation is constructed by means of decomposition of the signal f over a set of waveforms generated by translating (u) and scaling (s) one function- wavelet ψ, possibly well concentrated in time and frequency:

$$c_{s,u} = < f, \psi_{s,u} >, \quad \psi_{s,u} = \frac{1}{\sqrt{s}} \psi\left(\frac{t-u}{s} \right) \qquad (1)$$

The linear decomposition of signals using WT was a significant improvement over the windowed Fourier transform (WFT), allowing for orthogonal representation, fast numerical implementations and multiresolution decomposition of signals (Mallat 1989). WT has been successfully applied to the analysis of time-locked EEG phenomena (evoked potentials), where it's main drawback - sensitivity of the representation to the time shift of analyzed window (Durka 1996) - is not a serious problem. However, neither WT nor WFT provides enough resolution and flexibility in a general case, like description of transients occurring more or less randomly in time.

A high resolution time-frequency representation of signal's energy can be constructed by Cohen's class transforms (Williams 1997); they all derive from the quadratic Wigner transform which can be expressed as:

$$W_f(t,\omega) = \int f\left(t + \frac{\tau}{2} \right) \overline{f\left(t - \frac{\tau}{2} \right)} e^{-i\omega\tau} d\tau \qquad (2)$$

This representation satisfies the time and frequency marginals, but contains severe cross terms between different time-frequency structures, which may lead to mis-

interpretation. Sophisticated mathematics applied to reduce this effect created a class of Reduced Interference Distributions (see e.g. Williams (1997)), where reduction of cross terms is usually achieved at the cost of marginal properties.

In spite of the high resolution offered by Cohen's class transforms, their application is practically limited to visual inspection of time-frequency plots for each analyzed data epoch. A method which allows for parametric - fully quantitative - description of signals in time-frequency space is Matching Pursuit (MP), a method based on adaptive approximation of time series by functions chosen for each analyzed epoch. The MP was introduced by Mallat and Zhang (1993). The first application to biological signal concerned EEG analysis (Durka and Blinowska 1995). In the following we will describe the MP method itself, then point out some of the limitations of the original approach, and finally present a way of overcoming the bias of the original method. Properties of MP parametrization will be demonstrated on the example of sleep EEG; however the method is suitable for all kinds of signals, in particular non-stationary time series.

METHODS

The method relies on the approximation of the signal by functions (time-frequency atoms) chosen from a very large and redundant set. Given a set of functions (dictionary) $\{G=\{g_1,g_2,...,g_n\}$ such that $\|g_i\|=1$, we can define an optimal M -approximation as an expansion minimizing the error ε of the approximation of signal f by M atoms. Such an expansion is defined by the set of indices $\{\gamma_i\}_{i=1...M}$ of the chosen functions g_{γ_i} and their weights w_i:

$$\varepsilon = \left\| f(t) - \sum_{i=1}^{M} w_i g_{\gamma_i}(t) \right\| = \min \qquad (3)$$

Finding such an optimal approximation is computationally intractable (Davis 1994). Another problem emerges from the fact that such an expansion would be unstable with respect to the number M of used waveforms: changing M even by one can completely change the set of waveforms chosen for the representation. These problems turn our attention to sub-optimal solutions. A sub-optimal expansion, stable with respect to the number of chosen waveforms, can be found by means of an iterative procedure, such as the Matching Pursuit algorithm proposed by Mallat and Zhang (1993). A similar approach was discussed by Qian et al. (1992).

Matching Pursuit algorithm

MP (introduced in Mallat and Zhang (1993)) is an iterative, non-linear procedure which decomposes a signal into a linear expansion of waveforms chosen from a redundant dictionary. In the first step, a waveform g_{γ_o} best matching the signal f is chosen, and in each consecutive step waveform g_{γ_n} is matched to the signal's residuum $R^n f$, left after subtracting results of previous iterations:

$$\begin{cases} R^0 f = f; \\ R^n f = < R^n f, g_{\gamma_n} > g_{\gamma_n} + R^{n+1} f; \end{cases} \qquad (4)$$
$$g_{\gamma_n} = \arg\max g_{\gamma_i} \in G \left| < R^n f, g_{\gamma_i} > \right|$$

Orthogonality of $R^{n+1} f$ and g_{γ_n} in each step implies energy conservation:

$$\|f\|^2 = \sum_{n=0}^{m-1} \left| < R^n f, g_{\gamma_n} > \right|^2 + \left\| R^m f \right\|^2 \qquad (5)$$

If the dictionary is complete, which is usually the case, the procedure converges to f, i.e.

$$f = \sum_{n=0}^{\infty} < R^n f, g_{\gamma_n} > g_{\gamma_n} \qquad (6)$$

Discrete dyadic Gabor dictionary

A waveform (atom) from a time-frequency dictionary can be expressed as a translation (u), dilation (s) and modulation (ω) of a window function $g(t) \in L^2(R)$

$$g_\gamma(t) = \frac{1}{\sqrt{s}} g\left(\frac{t-u}{s} \right) e^{i\omega t} \qquad (7)$$

Optimal time-frequency resolution is obtained for gaussian $g(t)$, which for the analysis of real-valued discrete signals gives a dictionary of Gabor functions (sine-modulated gaussians):

$$g_\gamma(n) = K(\gamma,\phi) e^{-\pi\left(\frac{n-u}{s}\right)^2} \sin\left(2\pi \frac{\omega}{N}(n-u) + \phi \right) \qquad (8)$$

The value of $K(\gamma,\phi)$ is such that $\|g_{\gamma,\phi}\| = 1$. Complete sampling of discrete parameters $u = 1...N, \omega = 1...N/2$, $s = 1...N$ where N is the signal's size in points, produces a huge dictionary even for a relatively small N. Therefore in the "classical" implementation proposed by Mallat and Zhang (1993) the dictionary's atom's parameters are chosen from dyadic sequences. For a discrete signal of length $N = 2^L$ sampling is governed by a new parameter - octave j (integer). Scale s, corresponding to

atom's width in time, is chosen from the dyadic sequence $s = 2^j$, $0 \le j \le L$. Parameters u and ω, corresponding to atom's position in time and frequency, respectively, are sampled for each octave with an interval $s = 2^j$.

The size of this dictionary (and the resolution of decomposition) can be increased by oversampling by $2^l (l \ge 0)$ the time and frequency parameters u and ω. The resulting dictionary has $O(2^{2l} N \log_2 N)$ waveforms, so the computational complexity increases with oversampling by 2^l. Time and frequency resolutions increase by the same factor:

$$\Delta t = 2^{-l\frac{2^j}{f_s}}, \qquad \Delta f = 2^{-l\frac{f_s}{2^j}} \tag{9}$$

where f_s is the sampling frequency of analyzed signal. Resolution is hereby understood as the distance between centers of dictionary's atoms neighboring in time or frequency, and depends on the octave j (scale $s = 2^j$). Scale s in turn corresponds to the width of an atom in time (and frequency). We can define the time width of a time-frequency atom as the half-width of the window function $g(t)$:

$$T_{1/2} = 2\frac{2^j}{f_s}\sqrt{\frac{\ln 2}{\pi}} \tag{10}$$

In spite of the oversampling, the algorithm still looks for a signal's expansion only over a relatively small subset of the possible dictionary's functions. Issues related to the particular structure of this subset will be discussed in the section "Stochastic dictionaries".

Time-frequency energy distribution

From equation (6) we can derive a time-frequency distribution of a signal's energy by adding Wigner distributions of selected atoms (Mallat and Zhang 1993). Calculating the Wigner distribution directly from equations (2) and (6) would yield

$$Wf = \sum_{n=0}^{\infty} \left| < R^n f, g_{\gamma_n} > \right|^2 W g_{\gamma_n} + \tag{11}$$

$$\sum_{n=0}^{\infty} \sum_{m=0, m \ne n}^{\infty} < R^n f, g_{\gamma_n} > \overline{< R^m f, g_{\gamma_m} >} W[g_{\gamma_n}, g_{\gamma_m}]$$

The double sum, containing cross Wigner distributions of different atoms from the expansion given in eq. (6) corresponds to the cross terms generally present in the Wigner distribution. One usually tries to remove these terms in order to obtain a clear picture of the energy distribution in the time-frequency plane. Removing these terms from eq. (11) is straightforward - we keep only the first sum; we can define a magnitude $Ef(t,\omega)$:

$$Ef(t,\omega) = \sum_{n=0}^{\infty} \left| < R^n f, g_{\gamma_n} > \right|^2 W g_{\gamma_n}(t,\omega) \tag{12}$$

The Wigner distribution of a single time-frequency atom g_γ satisfies

$$\int_{-\infty}^{+\infty} \int_{-\infty}^{+\infty} W g_\gamma(t,\omega) dt d\omega = \left\| g_\gamma \right\|^2 = 1 \tag{13}$$

Combining this with energy conservation of the MP expansion (eq. 6) yields

$$\int_{-\infty}^{+\infty} \int_{-\infty}^{+\infty} Ef(t,\omega) dt d\omega = \left\| f \right\|^2 \tag{14}$$

This justifies the interpretation of $Ef(t,\omega)$ as the energy density of $f(t)$ signal in the time-frequency plane.

An example: simulated signal with noise

In Figure 1a a simple signal is constructed from a continuous sine wave (A), a one-point discontinuity (Dirac's delta, B) and three Gabor functions (C, D and E) of the same time positions (C and D) or the same frequencies (D and E). Fig. 1b gives the time-frequency energy distribution obtained for this signal from MP decomposition by means of eq. (12). On the left of Fig. 1 b, c, d, energy is proportional to height; on the right it is proportional to shades of grey. The perfect representation of all the signal structures is due to the fact that the signal was constructed as a sum of dictionary's elements only.

In Figure 1c and 1d a white noise of energy twice and four times the signal's energy is added. In both cases the same realization of white noise was used (with different weights). Table I presents the parameters of the simulated time-frequency structures A-E compared to parameters of corresponding time-frequency atoms fitted by MP to the signals mentioned, with S/N ratio from ∞ (simulated signal *b* without noise) through 1/2 (- 3 dB, signal c) to 1/4 (-6 dB, signal *d*).

We can observe some characteristic properties of decomposition:

1. Sine wave retains its frequency up to the noisiest signal. However, even in the absence of noise additional shorter structures are fitted near the beginning and the end of the signal to account for border effects. In noisy signals the "infinite" sine tends to be explained by two shorter structures, due to border effects again.

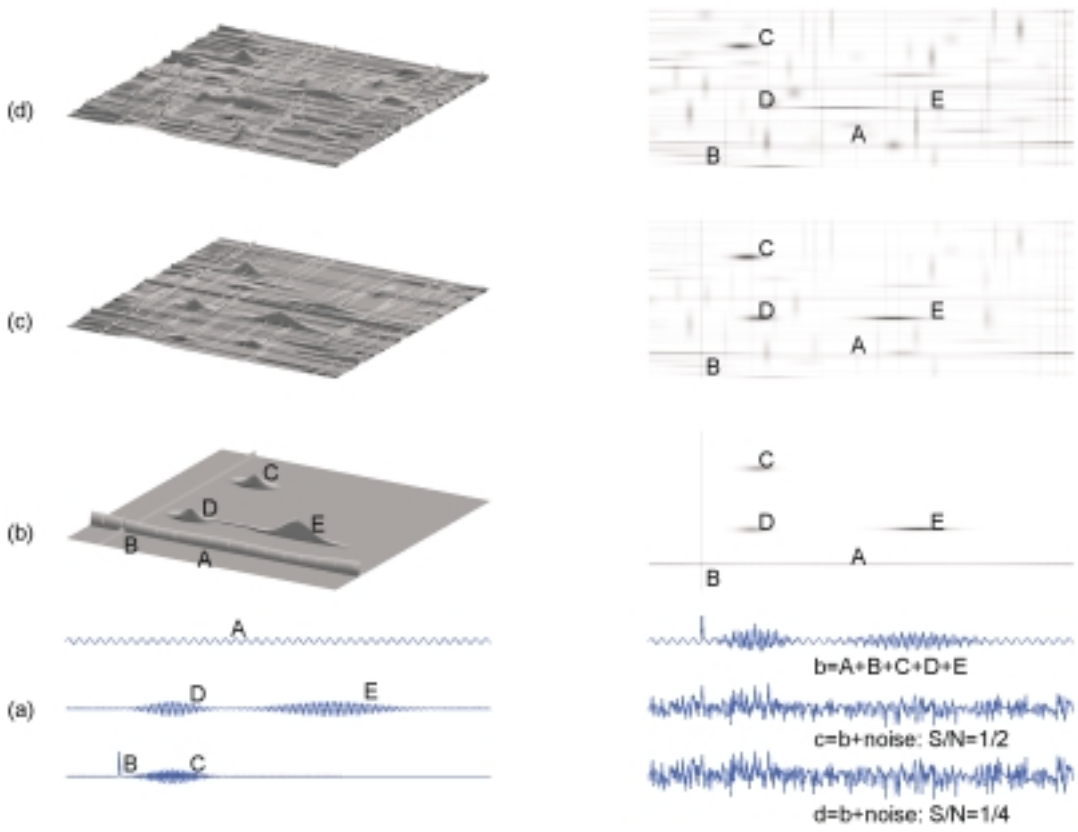

Fig. 1. (a): left - components of the simulated signal: sine A, Dirac's delta B and Gabor functions C, D and E. Right - signals, labelled b, c and d, constructed as sum of structures A-E and white noise, and decomposed in corresponding panels (b), (c) and (d). (b): time-frequency energy distribution (eq. 12) obtained for sum of structures A-E; in 3-D representation on the left energy is proportional to the height, in right panel - to the shades of gray. Panels (c) and (d): decompositions of signals with linear addition of noise, S/N = 1/2 (-3 dB) in (c) and -6 dB in (d), the same realization of white noise was used in both cases. Exact parameters of presented time-frequency structures are given in Table I.

2. Dirac's delta disappears in the strongest noise, but till then preserves its exact time position.
3. Gabor function C, being the only structure in this frequency, retains relatively well all of the parameters with a slight flow of time position at higher noise levels.
4. Finally, the two Gabor functions D and E lying at the same frequency with different time positions and widths exhibit slight flow of parameters for S/N=1/2. At higher noise levels they divide in to two longer structures: one in between (in Table I assigned to structure D) and one more to the right.

The above example demonstrates the robustness of the method in the presence of linearly added white noise - in this case most of the basic time-frequency characteristics were represented even in S/N=1/4 (- 6 dB).

Sleep spindles detection and analysis based upon Matching Pursuit parametrization

As described above, "classical" MP with a dyadic Gabor dictionary allows for computationally effective implementation, and hence was the first kind of MP architecture applied in biomedical signal processing. A study of sleep spindles, presented below, demonstrates the possibilities opened by the MP approach in EEG analysis.

Table I

Parameters of structures A-E (Fig. 1) - original values in simulated signal and parameters recovered by MP decomposition for signals with different S/N ratios. Time position of sine wave ([1]) and frequency of Dirac's delta ([2]) are set by convention as half of the time and frequency ranges, respectively

parameters	amplitude	scale	position	frequency
		structure A (sine)		
original	1.00	512	-	0.5000
S/N=∞	0.62	512	256[1]	0.5031
	0.98	256	506	0.5031
	0.9	256	14	0.5031
S/N=1/2	1.40	256	506	0.5031
	1.23	256	43	0.5031
S/N=1/4	1.41	256	506	0.5031
	1.16	256	43	0.5031
		structure B (Dirac)		
original	10.00	0	64	-
S/N=∞	10.37	0	64	1.57[2]
S/N=1/2	8.03	0	64	1.57[2]
S/N=1/4	-	-	-	-
		structure C (Gabor)		
original	3.00	64	128	2.40
S/N=∞	2.96	64	132	2.39
S/N=1/2	2.98	64	118	2.39
S/N=1/4	3.10	64	111	2.39
		structure D (Gabor)		
original	3.00	64	128	1.20
S/N=∞	2.96	64	124	1.19
S/N=1/2	2.75	64	132	1.19
S/N=1/4	1.72	256	234	1.18
		structure E (Gabor)		
original	3.00	128	320	1.20
S/N=∞	2.97	128	326	1.20
S/N=1/2	2.35	128	294	1.19
S/N=1/4	1.12	256	361	1.13

Experimental data

Overnight recordings of sleep EEG contained standard polysomnographic channels, 21 channels of EEG according to the 10-20 standard system (see insert in Fig. 5) and A1 and A2 derivations (ears). Silver electrodes were applied with collodion. Maximal accepted resistance was less than 5 Kohms. A 12 bit analog-digital converter was used with a conversion rate of 128 Hz (in some cases 102.4 Hz). Results described below were obtained from recordings of the second night's sleep of healthy volunteers, usually about 7 hours of EEG. Analysis was performed on signals referenced to the A1/A2 electrodes (linked ears). Subsequent segments of 20 s length were subjected to MP decomposition.

Choosing spindles from time-frequency atoms

Sleep spindles play a major role in the analysis of cerebral activity in sleep. Their morphology, described and defined mainly for the purpose of visual analysis (Rechtschaffen and Kales 1968), corresponds well to the basic shape of waveforms from the Gabor dictionary, so each spindle should be represented by one time-frequency atom. It remains to choose, from the waveforms fitted to the analyzed segment, those corresponding to sleep spindles. According to generally accepted criteria and our previous experience, time-frequency conditions for a structure to be considered a sleep spindle were defined as follows: frequency: 11-15 Hz, time width: 0.5-2 s (octaves 6-8, eq. 10). Amplitude presents a separate problem - in this study the threshold was set at 25 μV (min), based upon comparison of MP results with visual detection of sleep spindles. Time of occurrence and phase had no influence on discrimination, since information from different channels was treated separately.

Investigation of sleep spindles properties and distributions

The previous section defined a filter, which chooses from the atoms, fitted to the analyzed signal by a general MP procedure, those atoms corresponding to sleep spindles. Its application provides - in a completely automatic fashion - precise time-frequency parameters of all the sleep spindles present in a multichannel overnight EEG recording. For a clear visualization of this huge amount of information, several types of reports present parameters of selected atoms (or corresponding sleep spindles) in different coordinates. These reports are projections of multidimensional space of the spindle's parameters onto 2- (or 1-) dimensional subspaces, suitable for presentation of given phenomena.

Frequencies in frontal an parietal derivations

Figure 2 is composed from histograms of frequencies of sleep spindles plotted for each channel and placed on

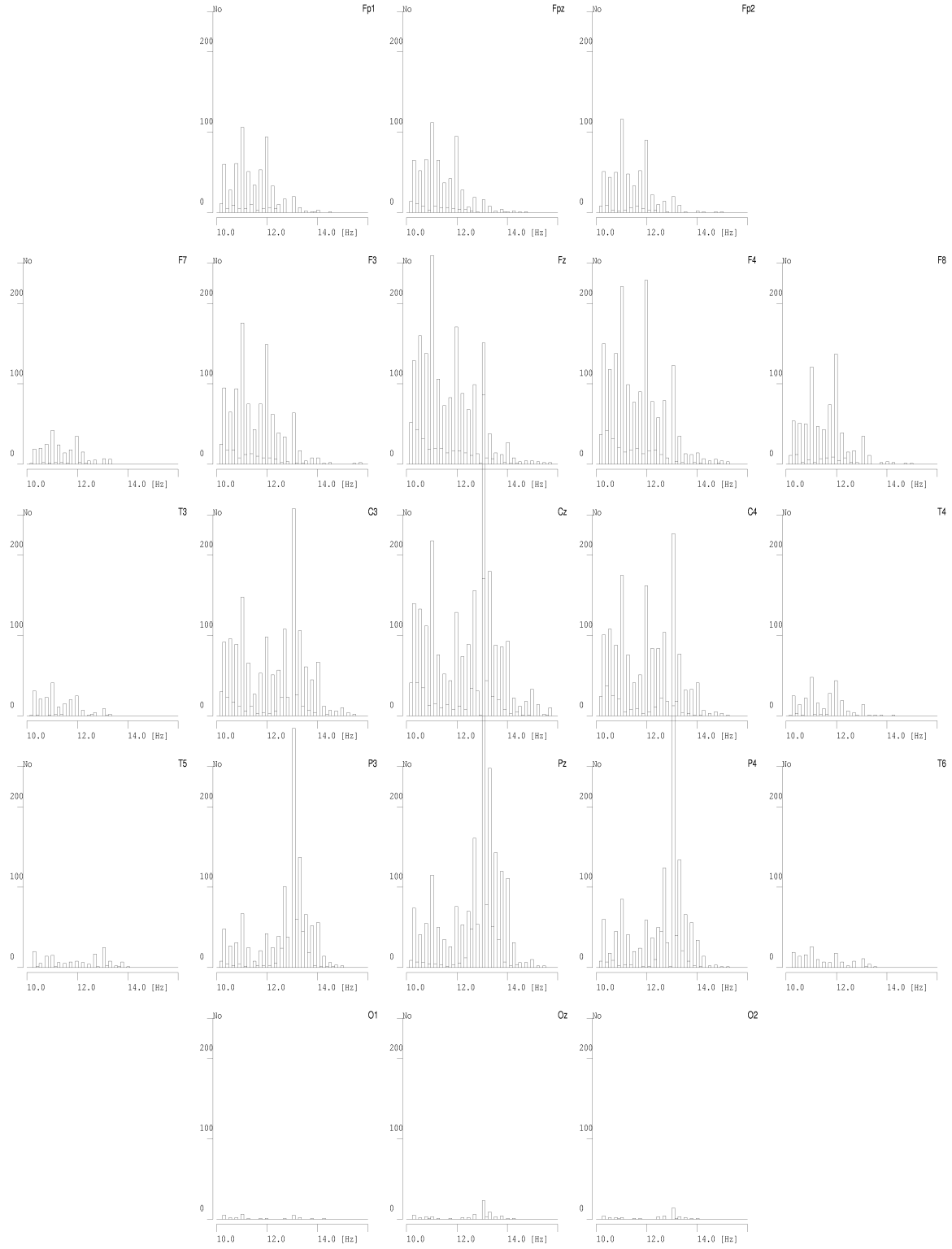

Fig. 2. Histograms of frequencies of sleep spindles detected in one overnight EEG recording. Plots are placed on page according to relative positions of corresponding derivations - front of head towards the top of page. We observe sparse occurences in peripheral (Fp*, O*, T* and F[7-8]) electrodes, therefore in the following multi-derivations plots (Figs. 3, 8 and 9) results only for the central 9 derivations (O*, C* and F[3, 4, z]) will be presented.

the page according to relative position of electrodes. We notice that higher frequencies are present in the more posterior, and lower in the more anterior derivations. This trend, present in all the analyzed recordings, conforms to the hypothesis of two generators of sleep spindles (Jankel and Niedermayer 1985, Jobert et al. 1992).

In Figure 3 each spindle is marked in frequency (horizontal) vs. amplitude (vertical) coordinates. Plots for

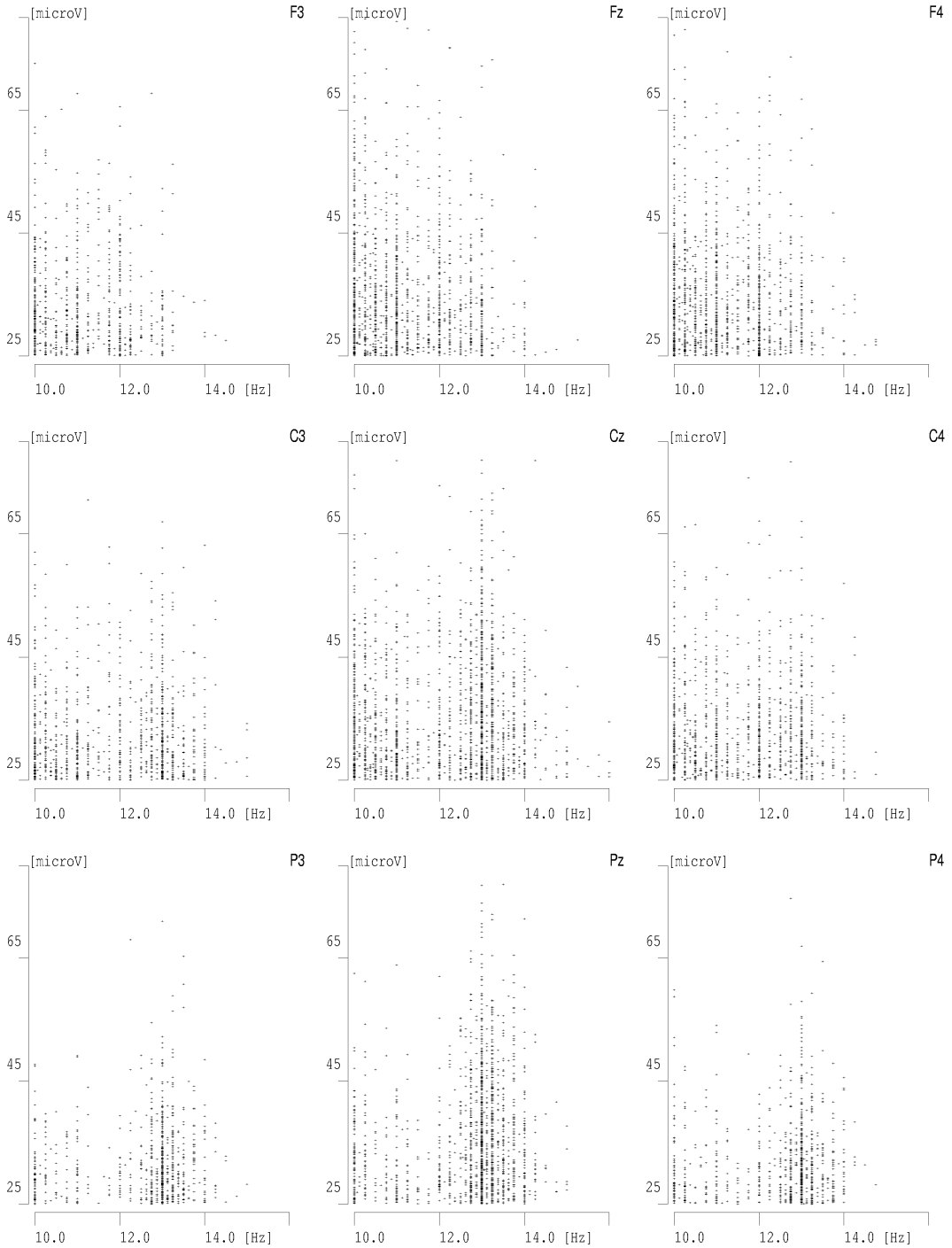

Fig. 3. Amplitudes of detected spindles (vertical) plotted *versus* their frequencies (horizontal) for the nine central derivations from Fig. 2.

each channel are positioned as in the previous figure. We observe for predominant frequencies higher amplitudes of spindles.

Superimposed spindles

In some cases a structure marked by an expert as one sleep spindle can have a frequency signature varying with time. Hao et al. (1992) interpreted such cases as a superposition of two different spindles. They applied complex demodulation to the structures marked especially for this purpose by an electroencephalographer.

Figure 4 presents a time-frequency energy distribution of 20 seconds of sleep EEG, where structures conforming to spindle's criteria are marked by the letters A-F. Structures C and D, as well as E and F, were classified as one spindle, i.e., their centers fell within a time section marked by the encephalographer as one spindle. Results of MP decomposition of these spindles can be interpreted in two possible ways: either we are dealing with different phenomena appearing closely together in time, or the frequency changes within the structure's duration. The structure of the changing frequency would be represented as several separate atoms, because in the applied dictionary there are only structures of constant frequency (compare Fig. 10).

Additional information can be provided by tracing the spatial distribution of these structures. Figure 5 presents the distribution of energy of spindles E and F across the electrodes. Each box corresponds to one recorded channel and contains (from the top): frequency [Hz], amplitude [μV], relative position in time [bottom left, ms] and time width [bottom right, ms] for a spindle possibly detected in each position. Boxes are positioned topographically as in Figs. 2-3, shading of each box is proportional to amplitude. We notice that higher-frequency spindle E is stronger in occipital electrodes, while amplitudes of lower-frequency spindle F are higher in frontal electrodes, although in some of them this spindle is missing. These distributions suggest that we are dealing with two different phenomena rather than one structure of changing frequency.

In the proposed framework, separation of superimposed structures with varying time-frequency signatures is straightforward. They can be automatically detected for the purpose of further investigations, based upon

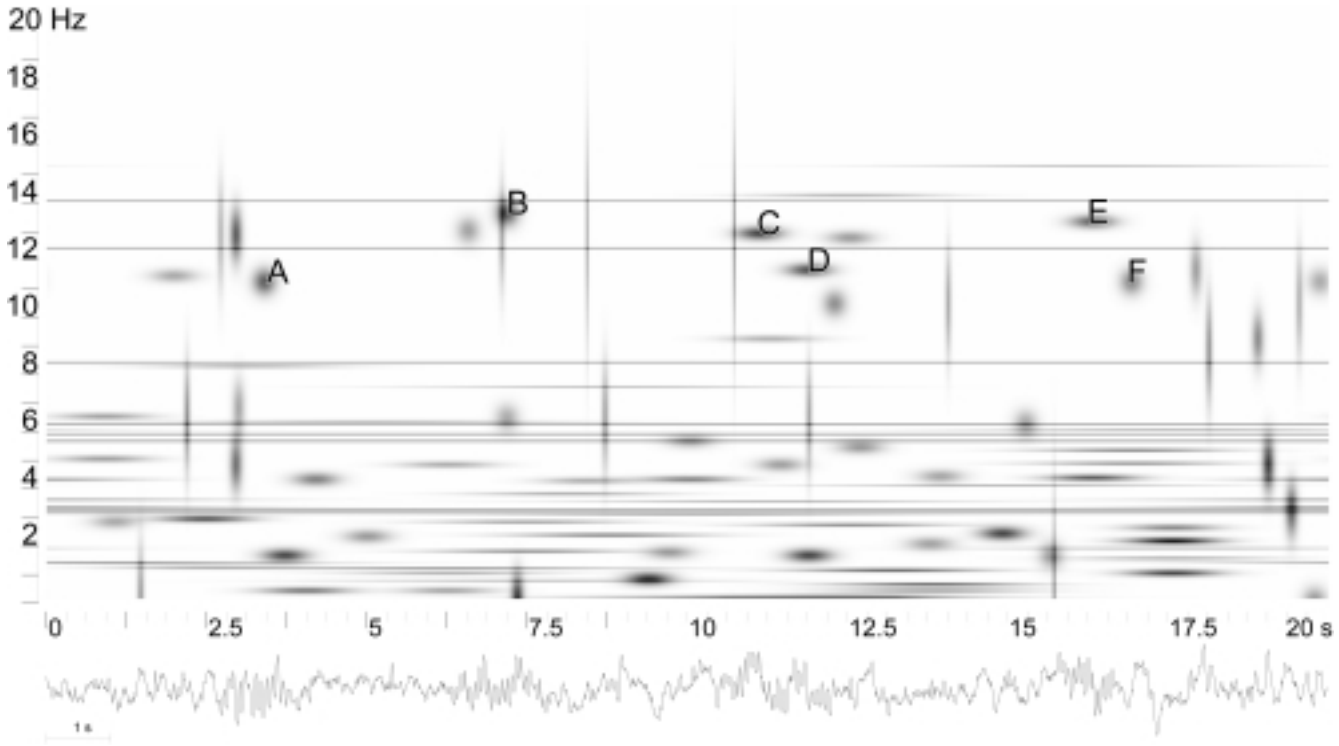

Fig. 4. Time-frequency energy distribution (equation 12) of 20 seconds of sleep EEG; structures corresponding to sleep spindles are marked by letters A-F. Structures C and D , as well as E and F, were classified as one spindle, i.e. their centers fell within a time section marked by the expert as one spindle.

proximity in time. In the work of Hao et al. (1992) each case of a superimposed spindles was identified visually, which limits the accuracy of the procedure and the possibility to process larger amount of data.

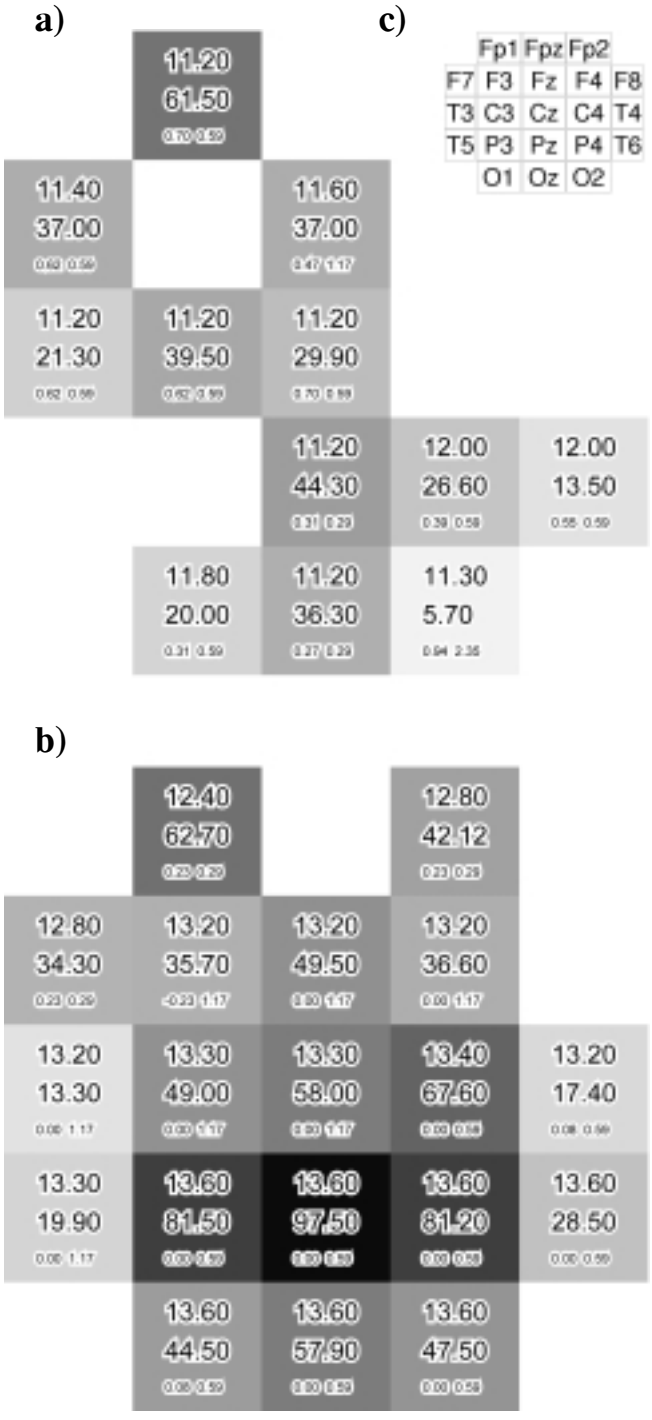

Fig. 5. Spindles F (upper plot) and E (lower plot) from Fig. 4 across channels. In each box, from top to bottom: frequency [Hz], amplitude [V], relative position in time [s], phase. Shades of gray proportional to the amplitude. Boxes positioned according to the corresponding electrodes from the 10-20. System shown in insert c).

A step towards complete description of sleep EEG

Reports discussed in previous sections were aimed at a simultaneous presentation of spindles detected in all EEG derivations. The time course of spindle occurrence in one channel, as presented in Fig. 6, relates directly to the classical perception of the sleep process - the "sleep staircase" or hypnogram (presented in Fig. 6a).

In order to provide a more complete picture, the time course of slow wave activity (SWA) is drawn simultaneously. Description of the SWA was traditionally assessed by spectral analysis. In the framework of MP we pick from the decomposition (already performed for the purpose of spindle parametrization) atoms conforming to the following criteria: frequency 0.5-4 Hz, amplitude > 75 μV and time span > 2.35 s.

Figure 6 presents the time course of spindles (b-d) and SWA (e-g) together with a hypnogram (a) in the same time scale. Data from the whole overnight recording is presented for the Pz electrode. Plots (b-c) show time distribution of frequencies and amplitudes of spindles, (d) gives the number of spindles detected per minute. Plots (f) and (g) give frequencies and amplitudes of SWA structures, while (e) presents the magnitude corresponding to the spectral power of structures classified as SWA, calculated for each minute. The time course of the spindle density is quite similar to the time course of the amplitudes of detected spindles. That means that in epochs where more spindles are detected, usually also higher--amplitude spindles are present (compare also Fig. 3). The time course of spindle activity and SWA in slow-wave sleep episodes [stages 3-4 on hypnogram] conforms to their previously recognized inverse relationship (Aeschbach and Borbély 1993).

This example demonstrates how easily MP parametrization can be extended to describe any time--frequency phenomena. Description of SWA was achieved by a direct implementation of it's generally acknowledged time-frequency characteristics. Since the MP decomposition is a general procedure, we do not have to repeat this time-consuming step to parametrize each new kind of structure. Construction of filters, choosing from the fitted atoms those corresponding to structures of interest, in many cases can be directly based upon "classical" knowledge of the EEG, formulated in

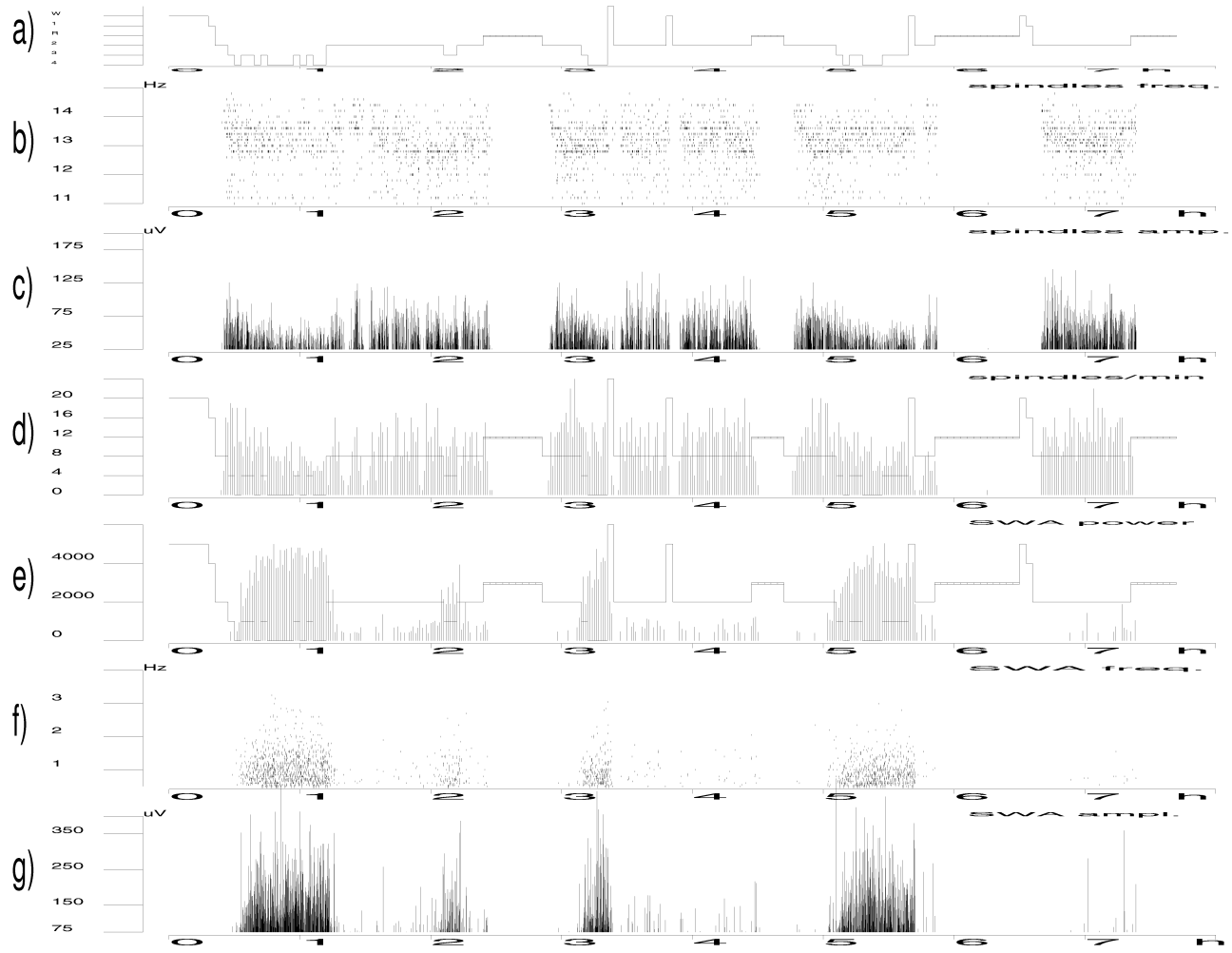

Fig. 6. Hypnogram a) and time course - on the same horizontal scale - of: b) frequencies and c) amplitudes of detected spindles, d) spindle density [1/min], e) SWA power, f) and g) frequencies and amplitudes of structures classified as SWA.

terms close to the time-frequency parameters. For a complete concordance with traditional methods, we can compute from MP parametrization a spectral power density estimate. In comparison to the traditional spectral estimates, this magnitude should reflect the investigated phenomena more accurately, since we take into account only the structures of interest, explicitly avoiding other structures of overlapping spectral characteristics.

Stochastic dictionaries

Closer investigation of Figs. 2 and 3 reveals - apart from the general finding of lower frequencies in frontal and higher in parietal derivations - a finer structure of local maxima. The question, of whether this is a property of the analyzed EEG or an artifact of the analysis method, provoked investigation of the statistical properties of MP decomposition as it related to the structure of the dictionary. These considerations, which finally led to the introduction of stochastic dictionaries, are presented in this section.

Influence of dictionary's structure on statistical properties of MP decomposition

In order to separate the problem of the algorithm's properties from the possible signal characteristics, we analyzed MP decompositions of 50 different realizations of white noise. Figure 7c presents a histogram of frequency centers of waveforms fitted to noise by MP decomposition over a dyadic dictionary. We observe high peaks in the middle of the frequency range, then in the

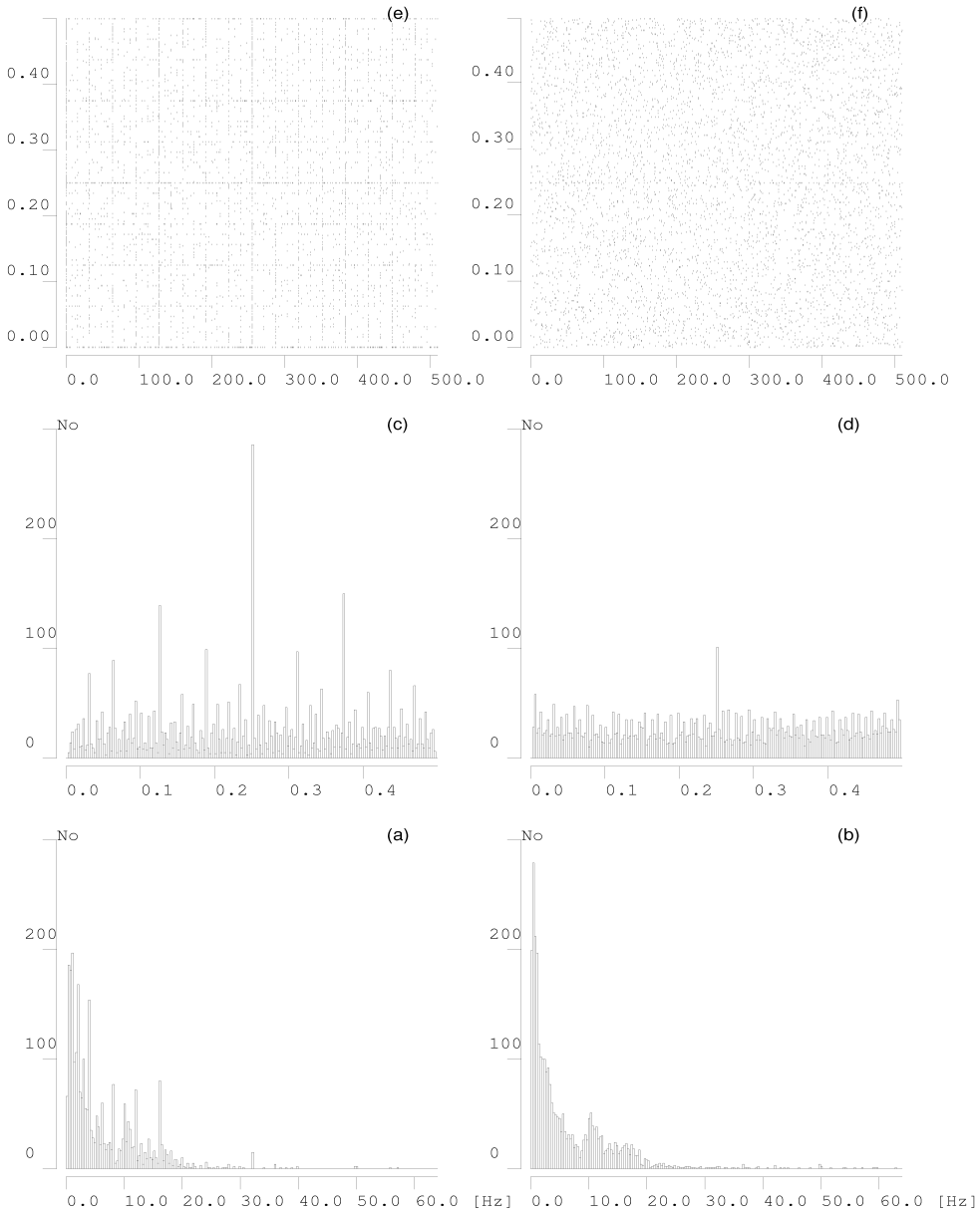

Fig. 7. Statistical properties of MP decomposition of 50 epochs of sleep EEG (a, b) and white noise (c-f) over dyadic (a, c, e) and stochastic (b, d, f) dictionaries. Histograms of frequency centers of atoms fitted by MP decomposition over dyadic dictionary to EEG (a) and noise (c) reveal additional structure, absent in corresponding decompositions performed over stochastic dictionaries b and d, respectively. Maximum in the middle of frequency range in panel d results from convention of assigning half of Nyquist frequency to Dirac's delta. In the top panel centers of atoms fitted to white noise are given in the time-frequency plane for dyadic (left, e) and stochastic (right, f) dictionaries.

quarters etc. In the case of atoms fitted to actual EEG (Fig. 7a), observed structure is superimposed on spectral characteristics of the signal. The structure observed in the two lower plots on the left side of the Fig. 7 comes from the fact that for each realization of the signal the same time-frequency grid was used. In consequence, in the plot consisting of the several realizations, the privileged positions connected with the dyadic dictionary are observed.

Figure 7e presents centers of atoms from the discussed decompositions using the dyadic dictionary in time (horizontal) vs. frequency (vertical) coordinates.

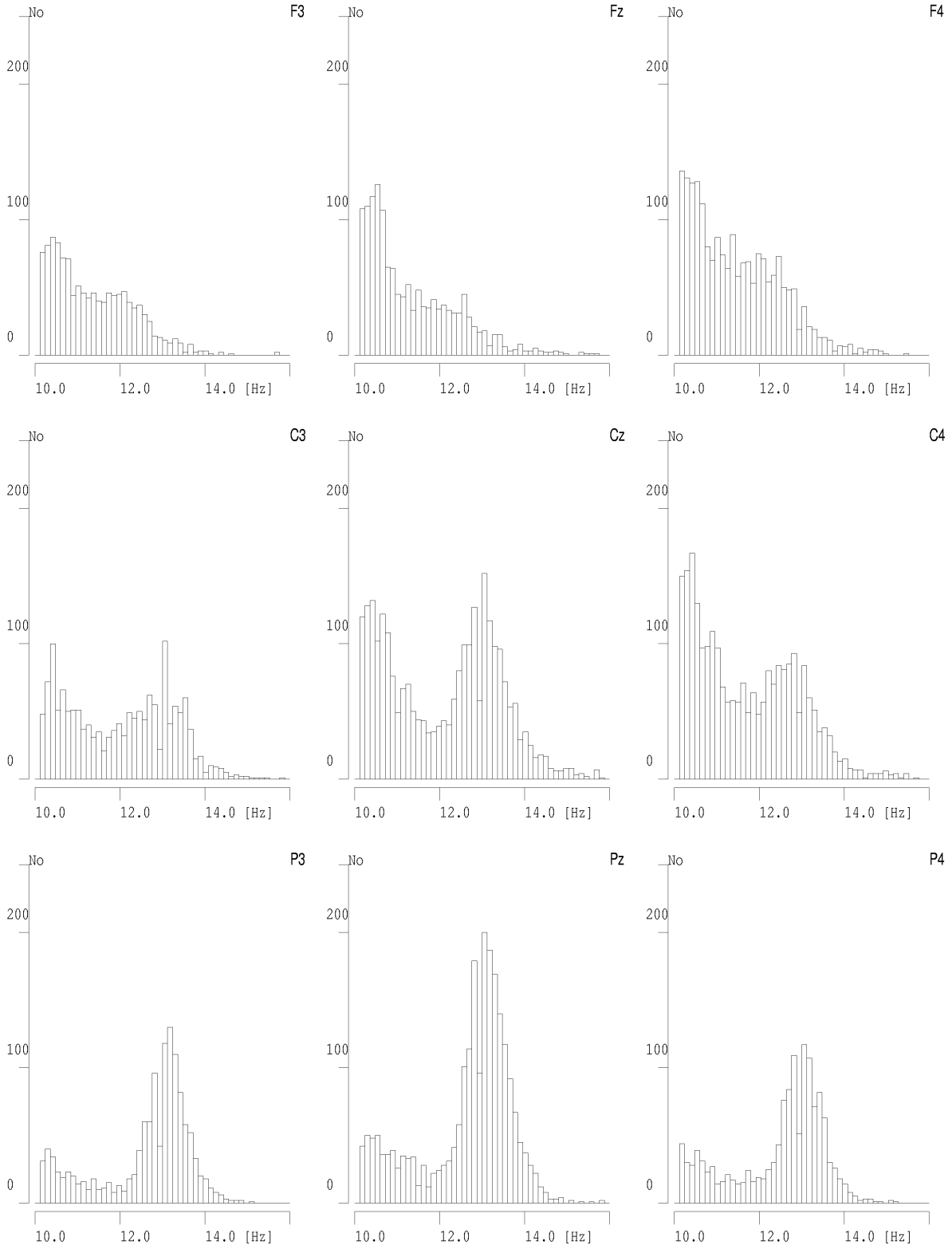

Fig. 8. Histograms of frequencies of sleep spindles detected in the same EEG recording as in Fig. 2, decomposed in stochastic dictionaries. Nine central derivations are presented.

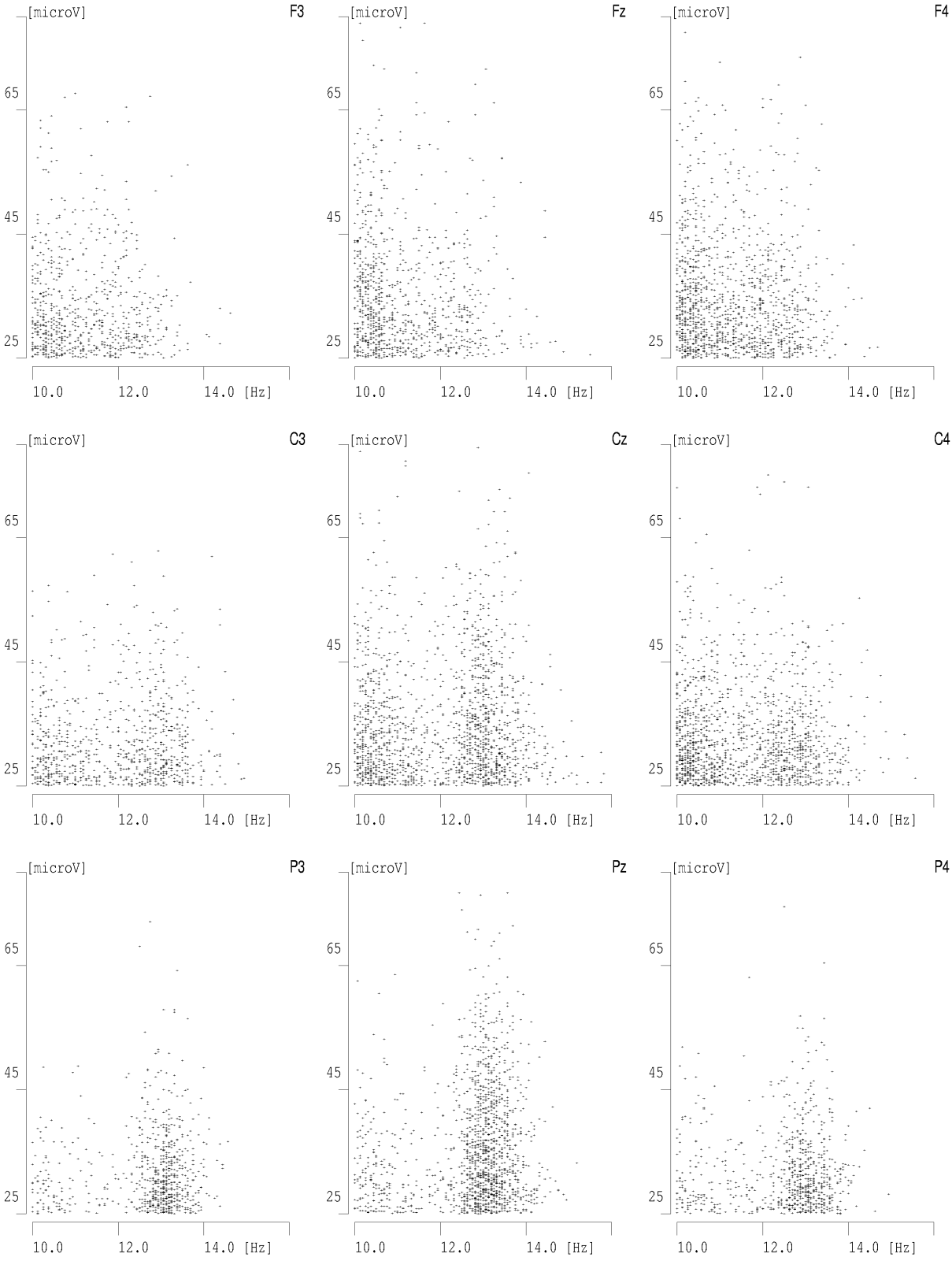

Fig. 9. Amplitudes of sleep spindles (vertical) plotted *versus* their frequencies (horizontal) detected in the same EEG recording as in Fig. 3 (as well as Figs. 2 and 8), based upon MP decomposition over stochastic dictionaries.

Due to a wide band of decomposed signals, the full structure of the dictionary can be observed. Higher density of atoms in certain regions of the dyadic dictionary (equation 8) "attracts" atoms chosen for decomposition.

Introduction of stochastic dictionaries

The previous section highlighted the influence of a dyadic dictionary structure on resulting MP decomposition. In fact, *any* structure of a dictionary, i.e. constant subsampling of the space of dictionary's atoms' parameters, will influence the statistical properties of the resulting decomposition. As a solution of this problem we propose MP with stochastic dictionaries. Instead of choosing some fixed positions of dictionary atoms (from dyadic or any other grid), we draw the parameters of Gabor functions from uniform distributions within the acceptable ranges, so that each signal's expansion is computed in a dictionary based on a different grid. The MP procedure based on stochastic dictionaries is more time-consuming than in case of dyadic dictionaries. However, recent developments in computer technology decrease the importance of this problem.

Improvement of statistical properties of decomposition

Plots on the right side of Fig. 7 (b, d, f) are constructed from a statistically unbiased MP representation obtained by decomposition in stochastic dictionaries. The histo-

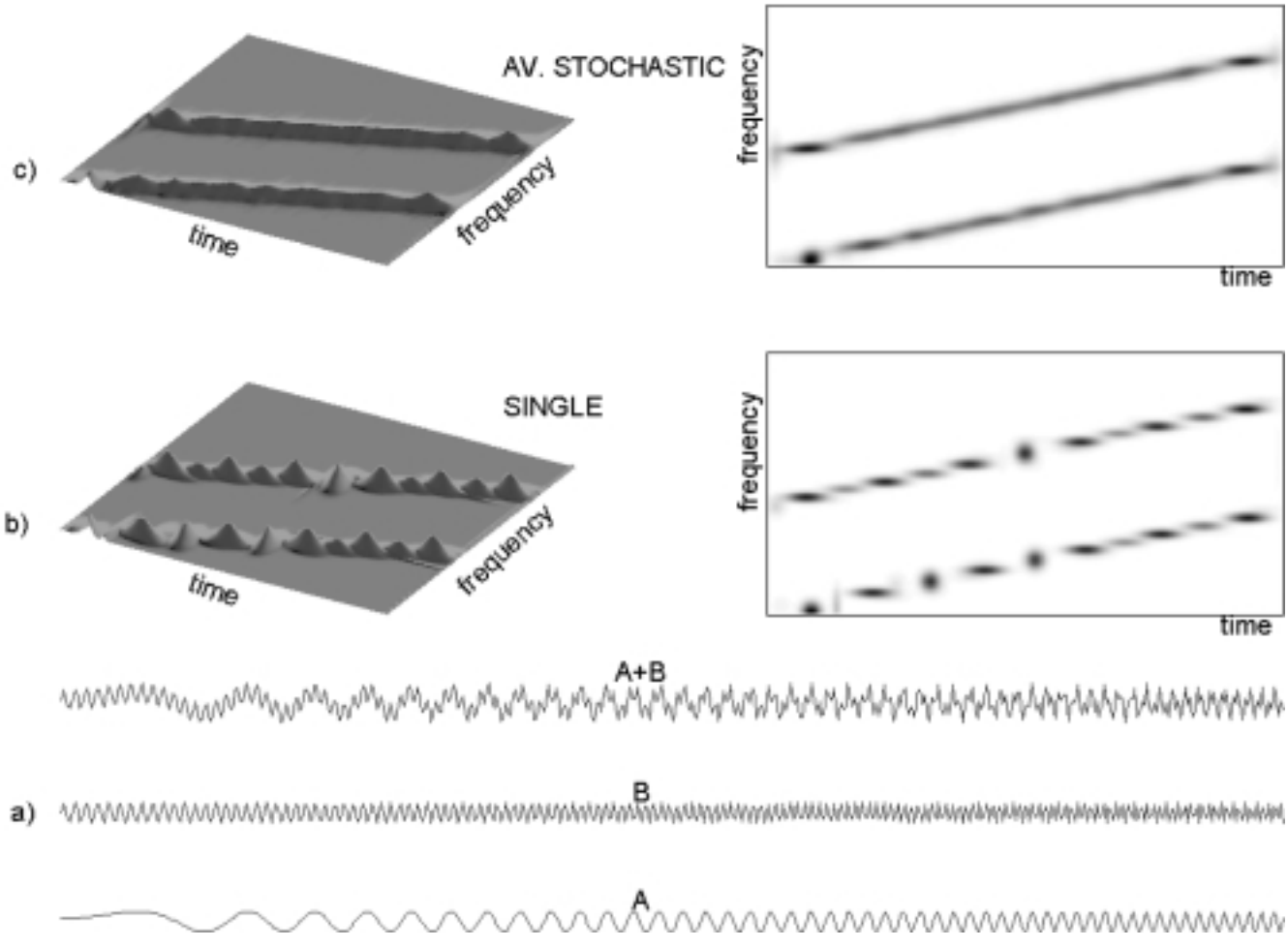

Fig. 10. Decomposition of signal composed of two chirps - sines of linearly changing frequency - presented in (a). In 3-dimensional plots on the left side energy is proportional to height, on flat pictures on the right - to the shades of gray. (b) presents results of a single decomposition over a dictionary consisting of 500,000 atoms, and (c) - time-frequency representation averaged over 50 realizations of smaller dictionary (15,000 atoms).

gram of frequencies in Fig. 7d (decomposition of white noise realizations) fluctuates around flat characteristics[1], while 7b gives a shape related to spectral characteristics of decomposed EEG[2].

Figure 7f presents centers of atoms, fitted to white noise realizations, in the time-frequency plane. Unlike the corresponding picture in 7e no particular structure is present, apart from the line in the half of Nyquist frequency, as discussed in the footnote.

Figures 8 and 9 present improvements of the distributions, shown in Figs. 2 and 3, achieved by decomposition of the same data over stochastic rather than dyadic dictionaries. The general trend, discussed in section "Frequencies in frontal an parietal derivations" is still clearly visible, while evenly distributed local maxima of spindle density disappeared, which proves that they were indeed artifacts of the algorithm.

Time-frequency distributions averaged over dictionaries

In the preceding section we have demonstrated how to avoid the bias of dictionary structure for averages estimated from multiple realizations. We can use averaging technique in case of a single data epoch with the aim of improvement of the time-frequency characteristics. A signal, which is particularly difficult to represent by means of MP, is a chirp (a sine with linearly changing frequency), since in the dictionary there are no waveforms of changing frequency. Such a signal has to be approximated by means of several waveforms. We can overcome this difficulty by decomposing the signal several times, each time over a dictionary with a different, randomly chosen grid. This procedure is presented on a signal composed from two chirps.

Figure 10b illustrates a decomposition of the signal (shown in 10a) over a dictionary containing 500,000 waveforms. We notice that structures of changing frequency are represented by a series of Gabor functions, since in the dictionary there are only structures of constant frequency. Figure 10c shows the average of 50 time-frequency maps, constructed from decompositions of the same signal over different realizations of smaller stochastic dictionaries, each of them containing 15,000 atoms. This result is closer to the expected representation than the single decomposition given in Fig. 10b. The computational cost need not to be higher than for a single decomposition, since in case of repetition of the procedure, dictionaries containing smaller number of atoms can be used. The problem of the density of the dictionary in the context of a quality of the decomposition is dicussed by Durka et al. (2001). The repetition of the decomposition over several stochastic dictionaries is recommended when a very accurate estimation of the frequency changes is of interest. In this particular case of chirp, better representation could have been obtained by a method aimed at chirps detection (e.g. Qian et al. 1998) or some of the time-frequency distributions discussed in the Introduction. Nevertheless, the proposed approach is a general one - it is by no means limited to a particular kind of structures and gives unbiased and free of cross terms estimates.

DISCUSSION

Matching Pursuit with a time-frequency dictionary of Gabor functions is a powerful and general tool for parametrization of non-stationary signals. The described applications to the analysis of sleep spindles and slow wave activity show new research possibilities opened by this approach in EEG analysis. The presented framework can be used for description of other signals structures. Apart from sleep spindles analysis, adaptive decomposition into Gabor functions (in its dyadic form) has been used for analysis of different signals: EEG recorded by depth and subdural electrodes (Franaszczuk et al. 1998), vibrotactile driving responses (Zygierewicz et al. 1998), vibroartrographic signals (Krishnan et al. 2000), phonocardiograms (Zhang et al. 1998) and otoacoustic emissions (Blinowska et al. 1997). The MP method has been recommended as an approach especially suitable for analysis of non-stationary signals (Lopes Da Silva 1999). The features, which make MP unique among other time-frequency methods are high resolution and parametric description of all kinds of data structures. No other method possesses both these properties. Continuous wavelet transform or Cohen's class transforms do not provide parametric description. Moreover Cohen's class transforms are biased by cross-terms. Discrete wavelet transforms give parametric descriptions, but their time-frequency resolution is severely limited. Presented in this work, MP with stochastic dictionaries re-

[1] peak in the middle stems from a convention of assigning half of Nyquist frequency to Dirac's delta (compare also Table I)

[2] Histogram in Fig. 7b is not an estimate of the average signal's spectrum, since frequency centers of fitted atoms were counted regardless of their amplitudes and frequency widths

moves bias of the original MP algorithm and further improves time-frequency resolution. It makes the presented method a unique tool for investigation of dynamic changes of brain activity.

A complete software package for Matching Pursuit with stochastic time-frequency dictionaries, used in this work, is available at .7exhttp://brain.fuw.edu.pl/mp.

ACKNOWLEDGEMENTS

We gratefully acknowledge Prof. Waldemar Szelenberger from Medical University of Warsaw for the EEG recordings and consultations. This work was partly supported by the State Committee for Scientific Research.

REFERENCES

Achermann P., Hartmann R., Gunziger A., Guggenbühl A. (1994) All night sleep and artificial stochastic control signals have similar correlation dimension. Electroencephalogr. Clin. Neurophysiol. 90: 384-387.

Aeschbach D., Borbély A. (1993) All-night dynamics of the human sleep EEG. J. Sleep Res. 2: 70-81.

Basar E., Bullock T.H. editors (1989) Brain dynamics, progress and perspectives. Springer-Verlag. 547 p.

Blinowska K.J., Durka P.J., Skierski A., Grandori F., Tognola G. (1997) High resolution time-frequency analysis of otoacoustic emissions. Technology and Health Care 5: 407-18.

Blinowska K.J., Malinowski M. (1991) Non linear and linear forecasting of the EEG time series. Biological Cybernetics 66: 159-165.

Davis G. (1994) Adaptive nonlinear approximations. PhD thesis, New York University. ftp://cs.nyu.edu/pub/wave/report/DissertationGDavis.ps.Z.

Dietsch G. (1932) Fourier-analyse von Elektrenkephalogrammen des Menschen. Pflüger's Arch. Ges. Physiol. 230: 106-112.

Durka P.J. (1996) Time-frequency analyses of EEG. PhD thesis, Warsaw University. ftp://brain.fuw.edu.pl/pub/DissertationPJDurka.ps.Z.

Durka P.J., Blinowska K.J. (1995) Analysis of EEG transients by means of matching pursuit. Ann. Biomed. Eng. 23: 608-611.

Durka P.J., Ircha D., Blinowska K.J. (2001) Stochastic time-frequency dictionaries for matching pursuit. IEEE T. Signal Proces. 49: 507-510.

Dvorák I. Holden A.V. editors (1991) Mathematical approaches to brain functioning diagnostics. Proceedings in Nonlinear Science. Manchester University Press. 463 p.

Franaszczuk P.J., Bergey G.K., Durka P.J., Eisenberg H.M. (1998) Time-frequency analysis using the matching pursuit algorithm applied to seizures originating from the mesial temporal lobe. Electroencephalogr. Clin. Neurophysiol. 106: 513-521.

Hao Y.L., Ueda Y., Ishii N. (1992) Improved procedure of complex demodulation and an application to frequency analysis of sleep spindles in EEG. Med. Biol. Eng. Comp. 30: 406-412.

Jankel W.R., Niedermayer E. (1985) Sleep spindles. J. Clin. Neurophysiol. 2: 1-35.

Jobert M., Poiseau E., Jahnig P., Schulz H., Kubicki S. (1992) Topographical analysis of sleep spindle activity. Neuropsychobiology 26: 210-217.

Krishnan S., Rangayyan R.M., Bell G.D., Frank C.B. (2000) Adaptive time-frequency analysis of knee joint vibroarthrographic signals for noninvasive screening of articular cartilage pathology. IEEE Trans. Biomed. Engineering 47: 773-83.

Lopes Da Silva F.H. (1996) The generation of electric and magnetic signals of the brain by local networks. In: Comprehensive Human Physiology (Eds. R. Greger and U. Windhorst). Vol. 1. Springer-Verlag, p. 509-528.

Lopes Da Silva F.H. (1999) EEG analysis: theory and practice. In: Electroencephalography: basic principles, clinical applications and related fields (Eds. E. Niedermayer and F.H. Lopes Da Silva). IV ed. Williams and Wilkins, Baltimore, p. 1135-1163.

Mallat S. (1989) A theory of multiresolution signal decomposition: the wavelet representation. IEEE Transactions on Pattern Analysis and Machine Intelligence 11: 674-693.

Mallat S., Zhang Z. (1993) Matching pursuit with time-frequency dictionaries. IEEE T. Signal Proces. 41: 3397-3415.

Pijn J.P., Neerven J.V., Noest A., Lopes da Silva F.H. (1991) Chaos or noise in EEG signals: dependence on state and brain site. Electroencephalogr. Clin. Neurophysiol. 79: 371-381.

Qian S., Chen D., Chen K. (1992) Signal approximation *via* data-adaptive normalized gaussian functions and its applications for speech processing. In: Proceedings of ICASSP-92, San Francisco, CA, p. 141-144.

Qian S., Chen D., Yin Q. (1998) Adaptive chirplet based signal approximation. In: IEEE 1998 International Conference on ASSP, Vol. III, Seattle, Washington, p. 1781-1783.

Rechtschaffen A., Kales A. editors (1968) A manual of standarized terminology, techniques and scoring system for sleep stages in human subjects. US Government Printing Office.

Skarda C.A., Freeman W.J. (1987) How brain makes chaos in order to make sense of the world. Behav. Brain Sci. 10: 161-195.

Williams W.J. (1997) Recent advances in time-frequency representations: Some theoretical foundations. In: Time frequency and wavelets in biomedical signal processing (Ed.

M. Akay). IEEE Press Series in Biomedical Engineering. IEEE Press.

Zhang X., Durand L.G., Senhadji L., Lee H.C., Coatrieux J.L. (1998) Time-frequency scaling transformation of the phonocardiogram based on the matching pursuit method. IEEE Trans. Biomed. Engineering 45: 972-9.

Zygierewicz J., Kelly E.F., Blinowska K.J., Durka P.J., Folger S.E. (1998) Time-frequency analysis of vibrotactile driving responses by matching pursuit. J. Neurosci. Methods 81: 121-129.

Received 14 February 2001, accepted 31 May 2001